Employing LIBS Technology to Investigate the Thermal Influence on Plasma Parameter Analysis in Pb Metal Model

Nibras Mousa Dbayh[1], Muayyed Jabar Zoory[1*] and Alaa H. Ali[2]

[1]*Department of Physics, College of Science, Mustansiriyah University, Baghdad – Iraq*
[2] *Material research Dep. Ministry of Science and Technology, Iraq.*

, [*]*Corresponding author: muayyedjz@uomustansiriyah.edu.iq*

Received 20 April 2023, Accepted 10 May 2023, Published 31. Dec 2023

DOI: 10.52113/2/10.02.2023/1-8

ABSTRAC: This study involved creating billets by varying the ratio of one element while keeping the ratios of four other elements constant. The metals Fe, Pb, Zn, Al, and Ni were utilized in the samples. In the first sample, the ratio of Fe (1.111g) Pb(3.333g), Zn (1.111g) Al (1.111g) and Ni(1.111g). The LIBS method was employed to conduct spectral analysis on a sample composed of all five metals. there was thermal equilibrium inside the plasma, and the excitation temperature was determined by analyzing the Pb emission lines that were observable in the sample. The study found that specific heat capacity plays a significant role in whether temperatures decrease or increase.

Keywords: laser induced breakdown spectroscopy (LIBS), Heat capacity and density, specific heat capacity.

1. Introduction

Laser –induced breakdown spectroscopy(LIBS) This approach may be summed up as follows .Plasma is produced when a high-intensity laser pulse is used on a particular sample. The sample might be either a solid, liquid, or gas. A high-intensity laser pulse is focused on the target, where a significant quantity of energy is delivered, raising its temperature[1]. It melts, evaporates, and ionizes the material on the surface, and this leads to the formation of plasma because of the high energy applied to the sample. The plasma begins to expand and form through an ionized gas[2]. The excited electrons start to return to the ground level during this that, an energy difference occurs that leads to the emission of photons called the emission of the plasma spectrum, as each element of the periodic table has its own spectral imprint that differs from the spectrum of the other element[4]. Through these spectra, the materials in the sample can be characterized by means of optical detection devices. This technique has made tremendous achievements in laser technology and detectors, effective techniques for analyzing different materials and minerals [5]. One advantage of LIBS technology is that it depicts in detail the elements and basic structure, as well as the plasma, which can be diagnosed by measuring the temperature (Te) and the electron density (Ne) [6]. LIBS

technique can be considered an appropriate technique for a range of different applications[7]. It has high accuracy and also does not need sample preparation in advance and can be used to determine the chemical elements in various studies, including the study of soil knowing the age of the elements[9,10.11]. and their components in the fields of medicine, heritage culture, as well as measuring plasma parameters and determining the concentrations of elements in different materials [8]. Lead (Pb) is a heavy metal with a silvery-bluish color, it is malleable and tensile, it has low electrical conductivity, and good corrosion-resistant [8]. Table 1 represents some of the chemical and physical properties of lead and other elements.

Table (1): Physical properties of lead and some metals[8]

chemical element	melting point c	Mass number	specific heat capacity J/Kg .c
AL	660.25	27	900
Pb	327.6	207	128
Ni	1453	59	445
Fe	1535	56	450
Zn	419.73	65	389

2. Materials and Methods

A group of minerals were purchased in the form of powders of Fe, Al, Zn, Ni and Pb, and these materials were of high purity. After that, hose metals were mixed in different proportions by a mixing device, as shown in Table (2), and then we compressed the samples with a piston with A pressure of 10 tons, five samples of different concentrations, were obtained, then we cleaned each sample with ethanol, and the five samples were dried by entering them into a hot oven for one hour, at 100 C, The samples became ready for work.. After that, the five samples were subjected to the LIBS system where the laser used was a laser N d: YAG laser wavelength of (1064 nm) with a pulse width of 10 ns and the wavelength range was between (165 nm and 816 nm). The convex lens used to concentrate the laser beam on the target had a focal length of 10 cm, a fundamental diameter of 5 mm, a focused diameter of 0.9 mm and, a power intensity of (100 m J) for the laser pulse. Adding the sample to the sample holder involved an environment with Ambient air, after which the plasma's emission was gathered in front of the plasma, keeping an eye on the path of the laser beam. using an imaging lens with a diameter of 15 mm. and focused onto optical fiber type (SMA,905µ m/0.22 NA), which delivered the plasma light to the entrance slit of spectrum analyzer model with a (1200 Line/mm) grating and (50µ m) slit dimension. Through eq (1) [1], the plasma temperature was obtained and eq(2) [1], the electron density, was obtained. **KBT (ev)** $= \frac{(Ek-Ei)}{\ln(Ii*gk*Aki*\lambda ij/\ Ii*gi*Aji*\lambda ki)}$ **(1)**

Where **(**$A\ ki$ **)** is the transition probability **U** (**T**) is the partition function.(E_k) is the excited level Energy. ($T\ e$) is the temperature.(K) is The

Boltzmann constants.(ג) is the wavelength. For correct evaluation of the lines' wavelengths(ג), intensities (I), And Transition Probabilities(A_{ki})[1,12,13].

$$n_e \geq 1.6 * 10^{12} . T^{\frac{1}{2}} . (\Delta E)^3 \quad (2)$$

Where T (K) is the plasma temperature. And ΔE is the highest energy transition for which the Condition holds[1] .

Table(2): Mixed metals in different proportions

sample S1	mixing ratios
Al	14.583%
Pb	41.666%
Ni	14.583%
Fe	14.583%
Zn	14.583%
sample S2	**mixing ratios**
Al	14.583%
Pb	14.583%
Ni	14.583%
Fe	41.666%
Zn	14.583%
sample S3	**mixing ratios**
Al	41.666%
Pb	14.583%
Ni	14.583%
Fe	14.583%
Zn	14.583%
sample S4	**mixing ratios**
Al	14.583%
Pb	14.583%
Ni	41.666%
Fe	14.583%
Zn	14.583%
sample S5	**mixing ratios**
Al	14.583%
Pb	14.583%
Ni	14.583%
Fe	14.583%
Zn	41.666%

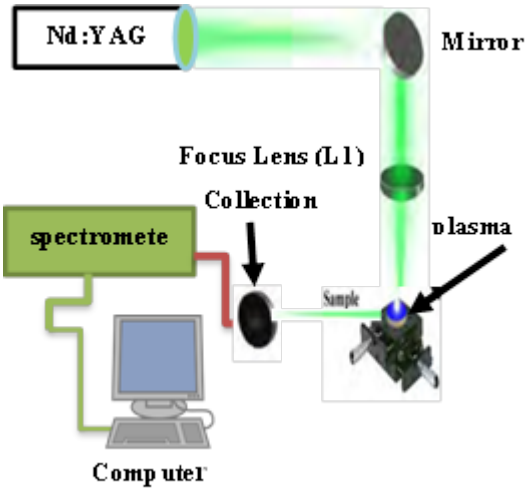

Figure 1: Schematic diagram of LIBS experimental setup

3.RESULTS AND DISCUSSION

3.1. SAMPLE ANALYSIS

An experiment involving five samples composed of varying amounts of Pb and other elements. was conducted. The combining of materials in different ratios, aimed to utilize LIBS (Laser-Induced Breakdown Spectroscopy) technology to identify the emission lines specific to Pb in each sample. To accurately determine the emission lines, we evaluated the spectra obtained from the samples and employed the atomic Spectra database provided by the National Institute of Calibration and Technology (NIST).Upon completion of the experiment, we collected a diverse range of wavelengths from the five samples. The wavelengths obtained using the LIBS approach are presented in tables labeled as 3, 4, 5, 6, and 7. The corresponding.

Table (3): Lines of Pb in sample 1.

λ(nm) LIBS	λ(nm) NIST	Intensity (a.u)	Aki (s^{-1}) Transition potential E+07	G_k	EK (cm-1) higher level energy
416.514	416.803	213.5583	12	5	45 443.17
240.285	240.193	236.4241	2.4	3	49 439.61
406.764	406.213	198.7016	9.2	3	46 068.438
367.401	367.149	317.5818	3.1	3	48 686.934
205.616	205.328	162.3619	1.02	3	48 686.934

Table (4): Lines of Pb in sample 2.

λ(nm) LIBS	λ(nm) NIST	Intensity (a.u)	Aki (s^{-1}) Transition potential E+07	G_k	EK (cm-1) higher level energy
416.514	416.803	203.4622	12	5	45 443.17
240.285	240.193	202.2143	2.4	3	49 439.61
406.764	406.213	270.9693	9.2	3	46 068.438
367.401	367.149	346.9902	3.1	3	48 686.934
205.616	205.328	175.0061	1.02	3	48 686.934

figures 2, 3, 4, 5, and 6, respectively. The main focus of our analysis was to determine the presence and concentration of the Pb element within these five samples.

In Figure(2) for the first sample, The wavelengths and intensities of Pb were obtained (416.51 nm Pb I) intensity(213.5 a.u) , (240.285 nm Pb I) intensity(236.42 a.u) , (406.76nm Pb I) intensity(198.70 a.u), (367.40 nm Pb I) intensity(317.58 a.u) ,(205.61 nm Pb I) intensity (162.36 a.u).

In Figure (3) for the first sample, The wavelengths and intensities of Pb were obtained (416.51 nm Pb I) intensity(203.46 a.u) (240.28 nm Pb I) intensity(202.21 a.u) , (406.76nm Pb I) intensity(270.96 a.u), (367.40 nm Pb I) intensity(346.99 a.u) ,(205.61 nm Pb I) intensity (175.00 a.u).

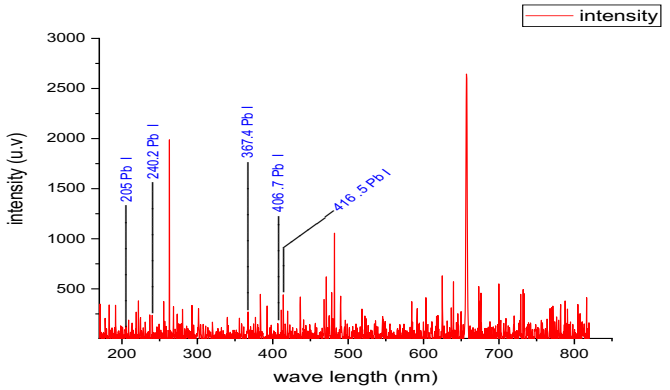

Fig. (2): Spectrum of sample 1.

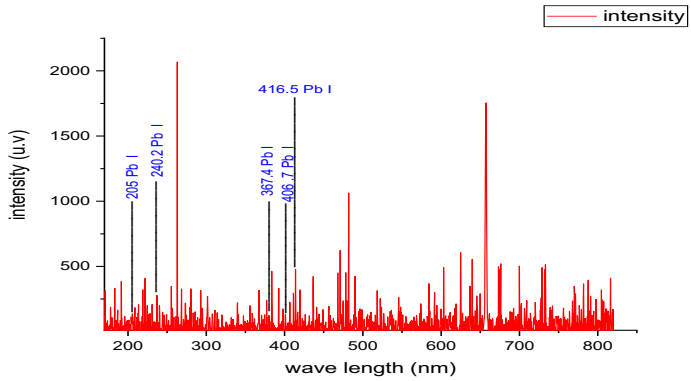

Fig. (3): Spectrum of sample 2.

Table (5): Lines of Pb in sample 3.

λ(nm) LIBS	λ(nm) NIST	Intensity (a.u)	Aki (s^{-1}) Transition potential E+07	G_k	EK (cm-1) higher level energy
416.514	416.803	234.906	12	5	45 443.17
240.285	240.193	245.2111	2.4	3	49 439.61
406.764	406.213	254.8094	9.2	3	46 068.438
367.401	367.149	347.8477	3.1	3	48 686.934
205.616	205.328	200.0178	1.02	3	48 686.934

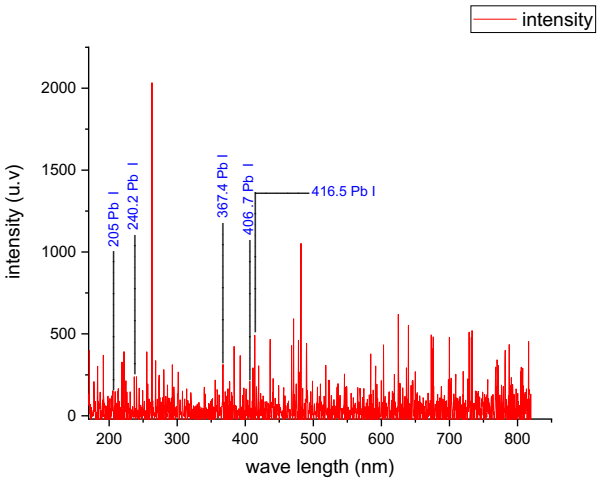

Fig. (4): Spectrum of sample 3.

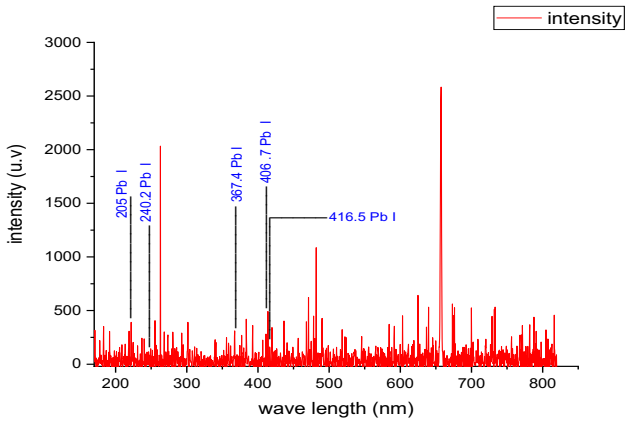

Fig. (5): Spectrum of sample 4.

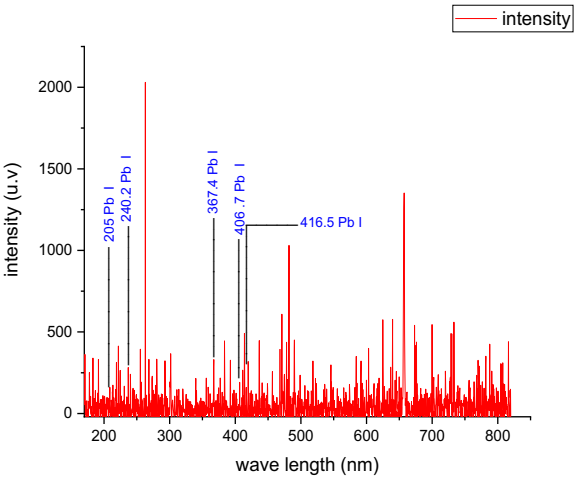

Fig. (6): Spectrum of sample 5.

In Figure (4) for the first sample, The wavelengths and intensities of Pb were obtained (416.51 nm Pb I) intensity(234.90 a.u) (240.285 nm Pb I) intensity(245.211 a.u) , (406.76nm Pb I) intensity(254.80 a.u), (367.40 nm Pb I) intensity(347.84a.u) ,(205.61 nm Pb I) intensity (200.01a.u).

Table (6): Lines of Pb in sample 4.

λ(nm) LIBS	λ(nm) NIST	Intensity (a.u)	Aki (s^{-1}) Transition potential E+07	G_k	EK (cm-1) higher level energy
416.514	416.803	217.3912	12	5	45 443.17
240.285	240.193	248.848	2.4	3	49 439.61
406.764	406.213	277.5783	9.2	3	46 068.438
367.401	367.149	381.0387	3.1	3	48 686.934
205.616	205.328	190.7059	1.02	3	48 686.934

In Figure (5) for the first sample, The wavelengths and intensities of Pb were obtained (416.51 nm Pb I) intensity(217.39 a.u) (240.28 nm Pb I) intensity(248.84 a.u) , (406.76nm Pb I) intensity(277.57 a.u), (367.40 nm Pb I) intensity(381.03 a.u) ,(205.61 nm Pb I) intensity (190.70 a.u).

Table (7): Lines of Pb in sample 5.

λ(nm) LIBS	λ(nm) NIST	Intensity (a.u)	Aki (s^{-1}) Transition potential E+07	G_k	EK (cm-1) higher level energy
416.514	416.803	200.3896	12	5	45 443.17
240.285	240.193	258.3448	2.4	3	49 439.61
406.764	406.213	233.0656	9.2	3	46 068.438
367.401	367.149	351.2574	3.1	3	48 686.934
205.616	205.328	153.398	1.02	3	48 686.934

In Figure (6) for the first sample, The wavelengths and intensities of Pb were obtained (416.51 nm Pb I) intensity(200.38 a.u) (240.28 nm Pb I) intensity(258.34a.u) , (406.76nm Pb I) intensity(233.06 a.u), (367.40 nm Pb I) intensity(351.25 a.u).using the saha-Boltzmann equation, the average electron temperature and

density of pb were obtained as shown in Table (8).

Table (8): represents the average temperature and electron density of Pb in the five samples.

samples	Element	temperature rate (K)	electron density rate
sample (S1)	Pb	2514.1	7.25937×10^{15}
sample (S2)	Pb	2518.3	7.26448×10^{15}
sample (S3)	Pb	2523.3	6.45984×10^{15}
sample (S4)	Pb	2527.8	7.28241×10^{15}
sample (S5)	Pb	2517.8	7.26472×10^{15}

In the first sample, through our observation of the average Temperature of Pb, which was (2514.1)K, and the Density of electrons (7.25937×10^{15}), while the mixing ratio for Pb metal was 41.666%. As for the second sample, the average temperature of Pb was (2518.3) K, and the electron density was (7.26448×10^{15}) the mixing ratio of Fe metal was 41.666% and in the third sample the temperature of Pb was (2523.3) K and the density of electrons was (6.45984×10^{15}) while the mixing ratio of Al metal was 20% and in the fourth sample the temperature of Pb became (2527.8)K and density electrons (7.28241×10^{15}) while the mixing ratio of Ni metal was 41.666%. In the fifth sample, the temperature of Pb was (2517.8)K and the density of electrons (7.26472×10^{15}) when the mixing ratio of Zn was 41.666%. As shown in Table (8)

3.2. DATA ANALYSIS

The first sample of Pb element exhibited an electron temperature (Te) of 2514.1 K and an electron density (Ne) of 7.25937E+15 when the lead percentage was 41.666%. With a specific heat capacity of 128 J/Kg·c, Pb showed a low thermal energy capacity. Increasing the mass or quantity of Pb resulted in a higher heat capacity, reducing its ability to absorb heat and subsequently decreasing its temperature. This also caused a decrease in the percentage of excited electrons escaping.In the second sample, Pb had an electron temperature (Te) of 2518.3 K and an electron density (Ne) of 7.26448×1015 when the lead percentage was 41.666%. The specific heat capacity of iron (Fe) was 450 J/Kg·c, indicating a high heat capacity. Increasing the mass led to an increased heat capacity, reducing Fe's ability to absorb heat. Other elements, including Pb, experienced an increase in temperature. The third sample yielded an electron temperature (Te) of 2523.3 K and an electron density (Ne) of 6.45984×1015 for Pb when the aluminum (Al) percentage was 41.666%. aluminum's heat capacity of 900 J/Kg·c is considered high. Increasing the mass resulted in a decreased ability of Al to absorb heat, while other elements, including Pb, exhibited higher temperatures. In the fourth sample, Pb had a temperature (Te) of 2527.8 K and an electron density (Ne) of 7.28241×1015 when the nickel (Ni)

percentage was 41.666%. The specific heat capacity of nickel was 445 J/Kg·c, indicating a high heat capacity. Increasing the mixing ratio led to a decreased heat absorption by nickel, causing an increase in the temperatures of other elements, including Pb. In the fifth sample, Pb displayed a temperature (Te) of 2517.8 K and a density (Ne) of 7.26472×1015 when the zinc (Zn) percentage was 41.666%. Zinc's specific heat capacity of 389 J/Kg·c was lower than that of other elements, resulting in greater heat absorption. As a result, the temperature of Zn increased while the temperatures of other elements, including Pb, decreased.

4. Conclusion

Based on the obtained results, it can be concluded that when the specific heat capacity of an element increases, its ability to absorb heat decreases. This indicates an inverse relationship between specific heat capacity and heat absorption ability. Therefore, an increase in specific heat capacity of a material results in a decrease in the ability to gain heat, leading to a decrease in temperature for Pb electrons. additionally, alloys offer the advantage of decreased thermal conductivity with an increase in mass. By introducing other elements to modify heat capacity, density, and specific heat capacity, it becomes possible to manipulate the plasma parameters of a specific metal, such as Pb, by adjusting the model parameters.

Acknowledgment. The authors would like to thank Mustansiriyah University (www.uomustansiriyah.edu.iq) Baghdad – Iraq for its support in the present work.

References

[1] Miziolek, A.W., V. Palleschi, and I. Schechter, 2006, Laser induced breakdown spectroscopy. Cambridge university press.

[2] Knight, A.K., et al., 2000, Characterization of laser-induced breakdown spectroscopy (LIBS) for application to space exploration. Applied Spectroscopy, 54(3), 331-340.

[3] Fu, H., et al., 2017. Calibration-free laser-induced breakdown spectroscopy (CF-LIBS) with standard reference line for the analysis of stainless steel. Applied Spectroscopy, 71(8), 1982-1989.

[4] Li, T., et al., 2012, Correction of self-absorption effect in calibration-free laser-induced breakdown spectroscopy (CF-LIBS) with blackbody radiation reference. Analytica Chimica Acta,. 1058, 39-47.

[5] Wei, K., et al., 2022, Application of Laser-Induced Breakdown Spectroscopy

Combined with Chemometrics for Identification of Penicillin Manufacturers. Applied Sciences,. 12(10), 4981.

[6] Tognoni, E., et al., 2010, Calibration-free laser-induced breakdown spectroscopy: state of the art. Spectrochimica Acta Part B: Atomic Spectroscopy, 65(1), 1-14.

[7] Jean-Noëla, M.K., K.T. Arthurb, and B. Jean-Marcc, 2020, LIBS technology and its application: overview of the different research areas. Journal of Environmental Science and Public Health, 4(3), 134-149.

[8] Zolotorevsky, V.S., N.A. Belov, and M.V. Glazoff, 2007, Casting aluminum alloys, 12. Elsevier Amsterdam.

[9] Kearton, B. and Y. Mattley, 2008, Sparking new applications. Nature photonics, 2(9), 537-540.

[10] Shen, X., 2009, Laser-induced breakdown spectroscopy with improved detection sensitivity, selectivity, and reliability. The University of Nebraska-Lincoln.

[11] Anabitarte, F., A. Cobo, and J.M. Lopez-Higuera, 2020, Laser-induced breakdown spectroscopy: fundamentals, applications, and challenges. International Scholarly Research Notices.

[12] Piñon, V., M. Mateo, and G. Nicolas, 2013, Laser-induced breakdown spectroscopy for chemical mapping of materials. Applied Spectroscopy Reviews, 48(5), 357-383.

[13] Mahdi, M., A. Ali, and M. Hussein, 2014. Using Laser-induced Breakdown Spectroscopy Technique to Identify the Low-Carbon Steel in the Industrial Alloy. Asian Journal Of Applied Science And Engineering, 3(2), 244-250.